International Journal of Engineering Research and Technology. ISSN 0974-3154, Volume 12, Number 6 (2019), pp. 802-808

The Evaluation of the Threshold Stress Intensity Factor and the Fatigue Limit of Surface-Cracked Specimen Considering the Surface Condition

Ki-Woo Nam[1], Won-Gu Lee[2] and Seok-Hwan Ahn[3,*]

[1,2] Department of Materials Science and Engineering, Pukyong National University, Busan 48513, Republic of Korea.

[3] Department of Aero Mechanical Engineering, Jungwon University, Chungbuk 28024, Republic of Korea.

Abstract

In this study, the threshold stress intensity factor and fatigue limit of surface-cracking materials were evaluated according to the variation of stress ratio and aspect ratio with reference to the fatigue limit of a gentle-grind specimen, severe-grind specimen, and shot-peened severe-grind specimen. Surface cracks in the gentle-grind, severe-grind, and shot-peened severe-grind specimens could be used to evaluate the threshold stress intensity factor and fatigue limit according to the stress ratio and aspect ratio using the equivalent crack length. As the surface crack length increased, the fatigue limit decreased rapidly at a small stress ratio and large aspect ratio. However, the depth of the surface cracks decreased rapidly at a small stress ratio and aspect ratio. As the surface crack length increased, the threshold stress intensity factor rapidly increased at a small stress ratio and large aspect ratio. However, the surface crack depth rapidly increased at a small stress ratio and aspect ratio. The reduction ratio of the fatigue limit at the surface crack length of the same stress ratio was larger than 0.4 at an aspect ratio 0.1. However, the surface crack depth was larger than 0.1 at an aspect ratio of 0.4. For a surface crack length of the same stress ratio, the rate of increase in the threshold stress intensity factor was smaller than 1.0 at an aspect ratio of 0.4; however, the surface crack depth was larger than 1.0 at an aspect ratio of 0.4. This is because when the aspect ratio became large, cracks propagated in the depth direction rather than the surface direction and at the same time when became similar to the surface crack length.

Keywords: threshold stress intensity factor, fatigue limit, stress ratio, aspect ratio, surface crack length, surface crack depth

1. INTRODUCTION

Most of the experiments to determine the fatigue crack growth rate and the threshold stress intensity factor were performed for large cracks and large through-wall cracks. As can be seen from actual fatigue failures, however, a failure occurs from very small cracks and is initiated by their growth. The importance of small cracks was recognized from scientific and practical perspectives, and it was found that small cracks do not follow the crack growth laws obtained from large cracks[1]. It was reported that the non-propagation of surface cracks is related to the constant threshold stress intensity factor for surface crack lengths larger than 0.5 mm [2]. For cracks smaller than 0.5 mm, it was not the threshold stress intensity factor but rather the stress identical to the fatigue limit that was the limit condition for very small defect propagation. For microcrack problems, the assumption of a small nonlinear domain does not hold. Haddad [3] introduced a valid formula for the dependency of the threshold stress intensity factor on the crack length by adding the microcrack length to the crack length. Moreover, Tange et al. [4] provided a more convenient formula for evaluating the threshold stress intensity factor by removing the microcrack length from the Haddad formula, and they conducted research on minimizing the damage to shot-peened welds caused by surface cracks using this formula and the Newman–Raju formula [5, 6-9]. Moreover, Ando et al. [10] presented a formula for evaluating the threshold stress intensity factor considering the size of the plastic zone, so that the fatigue limits and threshold stress intensity factors of all surface-cracking materials could be evaluated.

In this study, the threshold stress intensity factors and fatigue limits of surface-cracking materials were evaluated according to the stress ratio and surface crack aspect ratio with reference to the fatigue limits of the gentle-grind specimen, severe-grind specimen, and shot-peened severe-grind specimen [11], considering the machining process.

2. FRACTURE MECHANICS OF A SEMIELLIPTICAL SURFACE CRACK IN A FINITE PLATE

The fatigue limit and threshold stress intensity factor of a semielliptical surface crack in a finite plate can be evaluated as follows.

When a through-wall crack with a crack length of $2c$ in an infinite plate is subjected to the bending stress of σ_B, K can be calculated using Equation (1).

$$K = \sigma_B \sqrt{\pi c} \tag{1}$$

Meanwhile, the semielliptical surface crack K in a finite plate can be evaluated using the Newman–Raju formula [5]. As shown in Fig. 1, when a semielliptical surface crack with a surface crack length of $2c$ and a surface crack depth of a in

* *Corresponding author*

a finite plate is subjected to the uniform bending stress of σ_B, K can be obtained using Equation (2) [10].

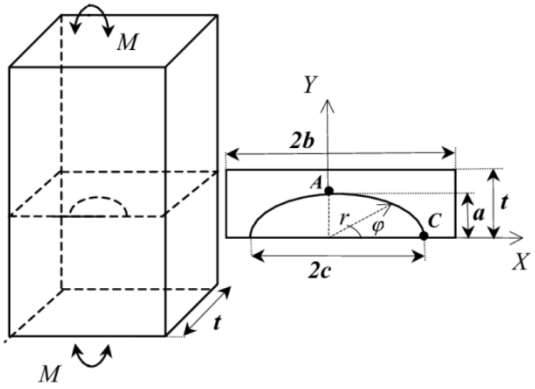

Fig. 1. Schematic illustration of a finite plate containing a semi-circular crack

$$K = \frac{H\left(\frac{a}{t},\ \frac{a}{c},\ \frac{c}{b},\ \emptyset\right)F\left(\frac{a}{t},\ \frac{a}{c},\ \frac{c}{b},\ \emptyset\right)}{\sqrt{Q\left(\frac{a}{c}\right)}}\ \sigma_B\sqrt{\pi a} = \beta\sigma_B\sqrt{\pi a} \qquad (2)$$

where, F and Q are geometrical correction functions, H is the correction function for the bending stress, t is the thickness of the finite plate, b is the half of the width of the finite plate, and $\emptyset$ is the angle of the tip of the semielliptical surface crack. β is the geometrical correction factor that integrated the geometrical correction functions. When the length of a through-wall crack in an infinite plate that represents the same K under the same stress is assumed to be the equivalent crack length c_e, Equations (1) and (2) become Equation (3).

$$K = \sigma_B\sqrt{\pi c_e} = \beta\sigma_B\sqrt{\pi a} \qquad (3)$$

Summarizing Equation (3), the relationship between c_e and a can be expressed as shown in Equation (4).

$$\sqrt{c_e} = \beta\sqrt{a} \qquad (4)$$

Therefore, the dependency of ΔK_{th}^R for the semielliptical surface crack in a finite plate on the crack length can be evaluated using Equation (5) derived by replacing c of Equation (1) with c_e of Equation (4).

$$\Delta K_{th}^R = 2\beta\Delta\sigma_\omega^R\sqrt{\frac{a}{\pi}}cos^{-1}\left\{\frac{\pi}{8\beta^2 a}\left(\frac{\Delta K_{th(l)}^R}{\Delta\sigma_\omega^R}\right)^2 + 1\right\}^{-1} \qquad (5)$$

where β is the function of $\emptyset$. The evaluation value of K varies depending on the angle of the crack tip that evaluates K. σ_ω^R is the fatigue limit of the plate, and $\Delta K_{th(l)}^R$ is the threshold stress intensity factor when a very long through-wall crack $2c_0$ exists in an infinite plate. The fatigue limit of a surface-cracking material ($\sigma_{\omega c}^R$) can be obtained using Equation (6), which was derived by substituting Equation (4) on the equivalent crack length into Equation (5) [10].

$$c_e\left\{sec\left(\frac{\pi\Delta\sigma_{\omega c}^R}{2\Delta\sigma_\omega^R}\right) - 1\right\} = \frac{\pi}{8}\left(\frac{\Delta K_{th(l)}^R}{\Delta\sigma_\omega^R}\right)^2 \qquad (6)$$

When a through-wall crack with a crack length of $2c$ exists in an infinite plate, however, the threshold stress intensity factor can be evaluated using Equation (7).

$$\Delta K_{th(c)}^R = \Delta\sigma_{\omega c}^R\sqrt{\pi c} \qquad (7)$$

In this case, $\Delta K_{th(l)}^R$ according to the stress ratio (R) is obtained using the ASME standard formula in Equation (8).

$$\Delta K_{th(l)}^R = \Delta K_{th(l)}^o\sqrt{(1-R)} \qquad (8)$$

The threshold stress intensity factor of a semielliptical surface crack can be obtained by substituting Equation (4) into Equation (7). When Equation (7) is applied to a semielliptical crack, it is the maximum value of K that determines ΔK_{th}. As K becomes largest when β is largest in Equation (2), the maximum value of β is substituted into Equation (5).

3. EVALUATION METHOD AND SPECIMENS

The production process is known to have significant effects on the fatigue characteristics of parts. Such effects are detrimental or beneficial, as shown in Table 1.

Table 1. Factors affecting the fatigue characteristics of parts

Detrimental	Beneficial
Hardening	Carburizing
Grinding	Honing
Machining	Polishing
Plating	Burnishing
Welding	Rolling
EDM and ECM	Shot peening

From a detrimental aspect, grinding, machining, and welding may cause metal fatigue cracks on the tensile surface. Curing, plating, and electrical discharge machining may a leave hard, brittle surface. Electrochemical machining may damage or weaken surface grain boundaries. From a beneficial aspect, all the listed processes induce compressive residual stress, thereby improving the fatigue life. Shot peening is most commonly used, because it provides the maximum compressive residual stress to various materials and parts.

Fig. 2 shows the S–N curves for various types of processing. The reference curve is for the case of the gentle-grind specimen, which showed a fatigue limit of 414 MPa. The severe-grind specimen showed a faster cutting speed and a larger cut. In this case, large surface tensile residual stress that lowers fatigue strength occurs because of fatigue. As the figure shows, the fatigue limit of the severe-grind specimen was 338 MPa, which was approximately 18% lower than that of the gentle-grind specimen. The final curve represents the fatigue limit of the shot-peened severe-grind specimen. The figure shows that this specimen exhibited a fatigue limit of 614 MPa, which was approximately 48% higher than that of the gentle-grind specimen. This increase in the fatigue limit occurred because the tensile residual stress caused by severe

grinding was changed to compressive residual stress by shot peening [7, 12-14].

Fig. 3 shows the relationship between the yield strength (σ_y) and threshold stress intensity factor $(\Delta K^0_{th(l)})$ of DNV F690 steel for offshore structures [15]. This is the relationship between σ_y and $\Delta K^0_{th(l)}$ obtained from various metal materials. As σ_y of DNV F690 steel is 850.32 MPa, $\Delta K^0_{th(l)}$ is found to be approximately 5.75 MPa$\sqrt{\text{m}}$ in the figure.

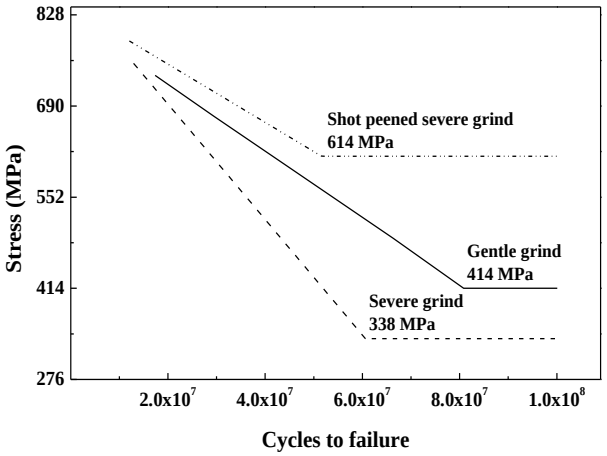

Fig. 2. S-N curves for various types of processing

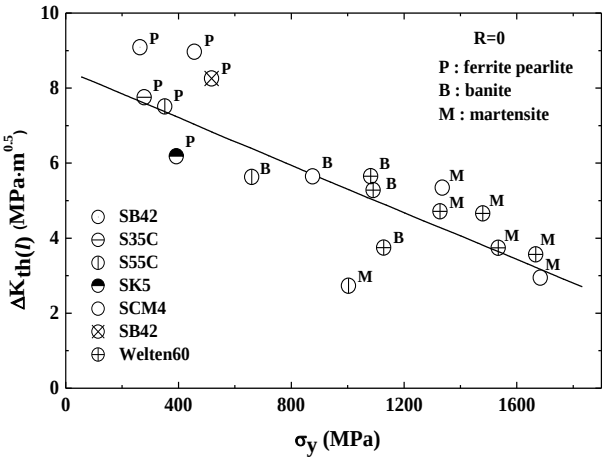

Fig. 3. Relationship between yield strength and threshold stress intensity factor

The specimens had a 50 mm width and a 10 mm thickness. Surface cracks were considered for the crack shapes, and the aspect ratio (*As*) was set to 1.0 and 0.4. The stress ratio (*R*) of the fatigue load was set to 0, 0.4, and 0.8, and a bending load was applied. The fatigue limit σ^0_ω used was 414 MPa for the gentle-grind specimen, 338 MPa for the severe-grind specimen, and 614 MPa for the shot-peened severe-grind specimen, as determined above.

The fatigue limit $(\sigma^R_{\omega(c,a)})$ of each surface-cracking material was obtained using Equation (6), and the result was substituted into Equation (7) to obtain $\Delta K^R_{th(c,a)}$. In this instance, it was assumed that the maximum stress according to the stress ratio was constant. Table 2 shows the conditions used in the evaluation.

Table 2. Conditions used in the evaluation

Stress ratio (R)	$\Delta K^R_{th(l)}$ (MPa$\sqrt{\text{m}}$)	Aspect ratio (As)	σ^0_ω (MPa)
0	5.75	1.0 4.0	· Gentle grind: 414 · Severe grind: 338 · Severe grind+ Shot peening : 614
0.4	4.45		
0.8	2.57		

4. RESULTS AND DISCUSSION

4.1 Relationship between the fatigue limit $(\sigma^R_{\omega c})$ and the crack dimensions for the surface-cracking materials

Figs. 4, 5, and 6 show the fatigue limit $(\sigma^R_{\omega(c,a)})$ values of the surface-cracking materials obtained from the gentle-grind, severe-grind, and shot-peened severe-grind specimens. In each figure, (a) represents the fatigue limit of the cracking material according to the surface crack length "*c*", and (b) represents the fatigue limit according to the surface crack depth "*a*". These were obtained using Equation (6).

The fatigue limit $(\sigma^R_{\omega 0})$ values of the gentle-grind specimen were 414, 248, and 83 MPa at stress ratios of 0, 0.4, and 0.8, respectively. The fatigue limit $(\sigma^R_{\omega 0})$ values of the severe-grind specimen were 338, 203, and 68 MPa at stress ratios of 0, 0.4, and 0.8, respectively. The fatigue limit $(\sigma^R_{\omega 0})$ values of the shot-peened severe-grind specimen were 614, 368, and 123 MPa at stress ratios of 0, 0.4, and 0.8, respectively. In this instance, the threshold stress intensity factors $(\Delta K^R_{th(l)})$ when a very long through-wall crack exists in an infinite plate were 5.75, 4.45, and 2.57 MPa, respectively.

Fig. 4(a) shows the relationship between the fatigue limit $(\sigma^R_{\omega c})$ and the crack length *c* for the gentle-grind specimen, while Figs. 5(a) and 6(a) show such relationships for the severe-grind specimen and the shot-peened severe-grind specimen, respectively. For each specimen, the same results were obtained as follows. For *R* = 0, the fatigue limit of each surface-cracking material decreased as the crack length increased, regardless of the aspect ratio (*As*), but it decreased more rapidly when As was 1.0 than when it was 0.4. For *R* = 0.4, a tendency similar to that of *R* = 0 was observed. For *R* = 0.8, however, the fatigue limit of each surface-cracking material decreased more slowly compared with the cases of *R* = 0 and *R* = 0.4.

Fig. 4(b) shows the relationship between the fatigue limit $(\sigma^R_{\omega a})$ and the crack depth *a* for the gentle-grind specimen, while Figs. 5(b) and 6(b) show such relationships for the severe-grind specimen and the shot-peened severe-grind specimen, respectively. For each specimen, the same results were observed as follows. For *R* = 0, the fatigue limit of each surface-cracking material decreased as the crack depth increased, as with the crack length, but it decreased more rapidly when the aspect ratio (*As*) was 0.4 than when it was 1.0. A similar tendency was observed for *R* = 0.4. For *R* = 0.8, however, the fatigue limit of each surface-cracking material

decreased more slowly compared with the cases of R = 0 and R = 0.4.

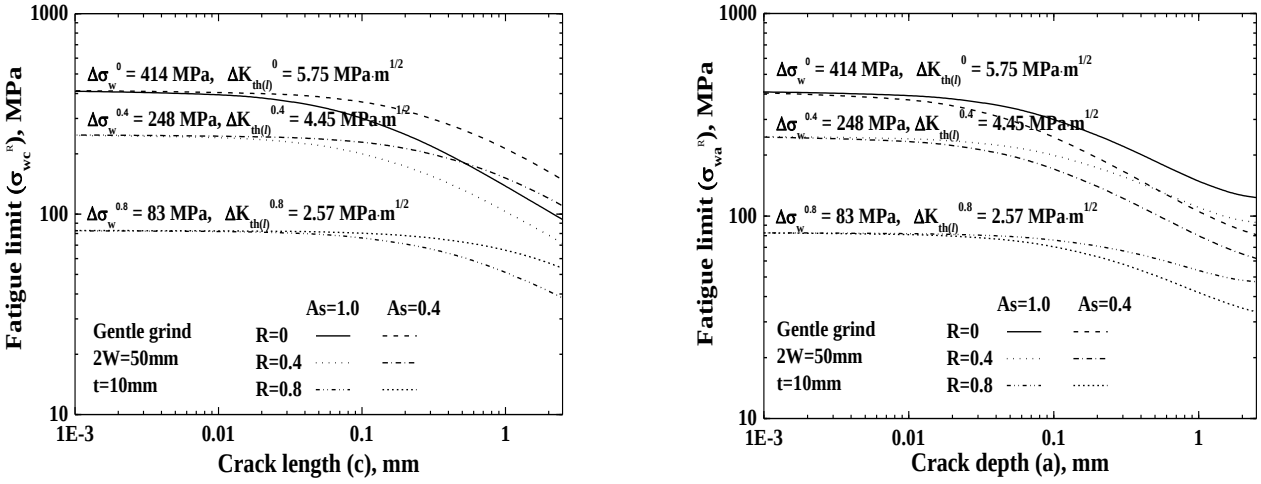

(a) (b)

Fig. 4. Fatigue limit according crack length (a) and crack depth (b) on gentle grind specimen

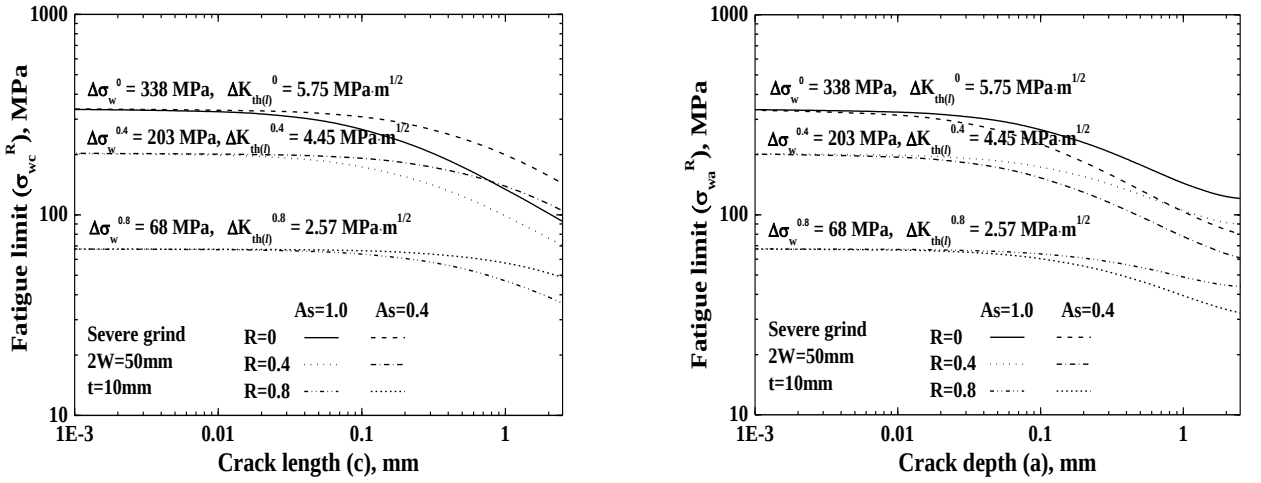

(a) (b)

Fig. 5. Fatigue limit according crack length (a) and crack depth (b) on severe grind specimen

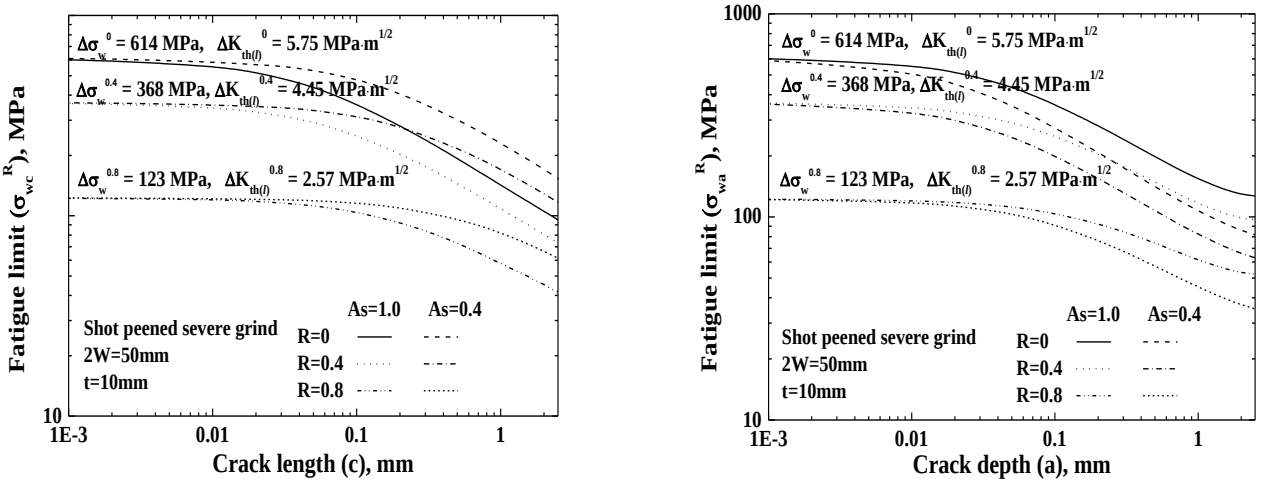

(a) (b)

Fig. 6. Fatigue limit according crack length (a) and crack depth (b) on shot peened severe grind specimen

4.2 Relationship between the threshold stress intensity factor $(\Delta K^R_{th(c,a)})$ and the crack dimensions for the surface-cracking materials

Figs. 7, 8, and 9 show the threshold stress intensity factors $(\Delta K^R_{th(c,a)})$ of the gentle-grind specimen, severe-grind specimen, and shot-peened severe-grind specimen according to the crack length and crack depth. In each figure, (a) represents the threshold stress intensity factor of each surface-cracking material according to the surface crack length "*c*", and (b) represents the threshold stress intensity factor according to the surface crack depth "*a*". These were obtained using Equation (7). The threshold stress intensity factors $(\Delta K^R_{th(l)})$ of the three specimens were 5.75, 4.45, and 2.57 MPa at stress ratios of 0, 0.4, and 0.8, respectively.

Fig. 7(a) shows the relationship between the threshold stress intensity factor $(\Delta K^R_{th(c)})$ and the crack length *c* for the gentle-grind specimen, while Figs. 8(a) and 9(a) show such relationships for the severe-grind specimen and the shot-peened severe-grind specimen, respectively. Each specimen exhibited the same results as follows. For $R = 0$, the threshold stress intensity factor increased as the crack length increased regardless of the aspect ratio (*As*), and it increased more rapidly when *As* was 1.0 than when it was 0.4. A similar tendency was observed for $R = 0.4$. For $R = 0.8$, however, the threshold stress intensity factor increased more slowly compared with the cases of $R = 0$ and $R = 0.4$.

Fig. 7(b) shows the relationship between the threshold stress intensity factor $(\Delta K^R_{th(a)})$ and the crack depth *a* for the gentle-grind specimen, while Figs. 8(b) and 9(b) show such relationships for the severe-grind specimen and the shot-peened severe-grind specimen, respectively. For each specimen, the same results were observed as follows. For $R = 0$, the threshold stress intensity factor increased as the crack depth increased as with the crack length, but it increased more rapidly when the aspect ratio (*As*) was 0.4 than when it was 1.0. A similar tendency was observed for $R = 0.4$. For $R = 0.8$, however, the threshold stress intensity factor increased more slowly compared with the cases of $R = 0$ and $R = 0.4$.

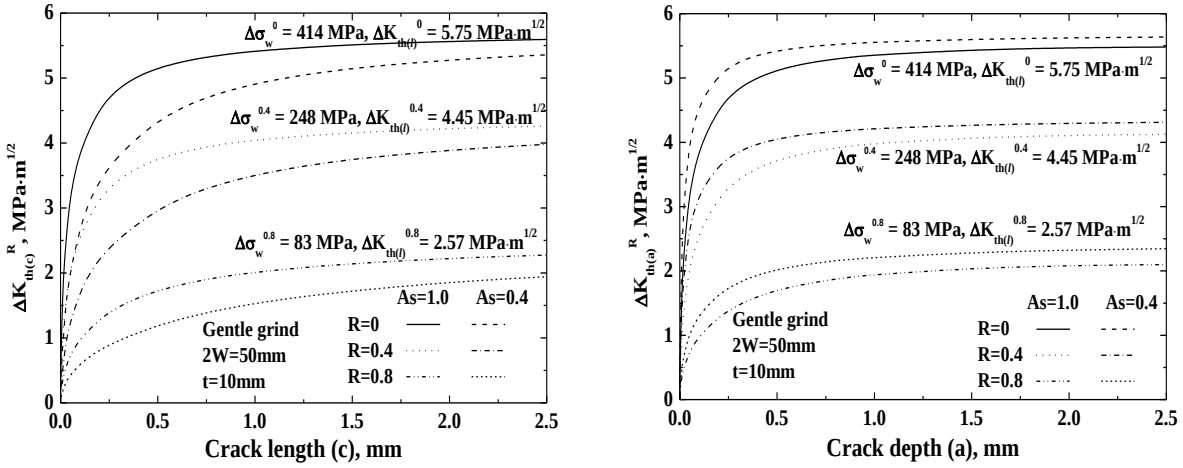

(a) (b)

Fig. 7. Threshold stress intensity factor according crack length (a) and crack depth (b) on gentle grind specimen

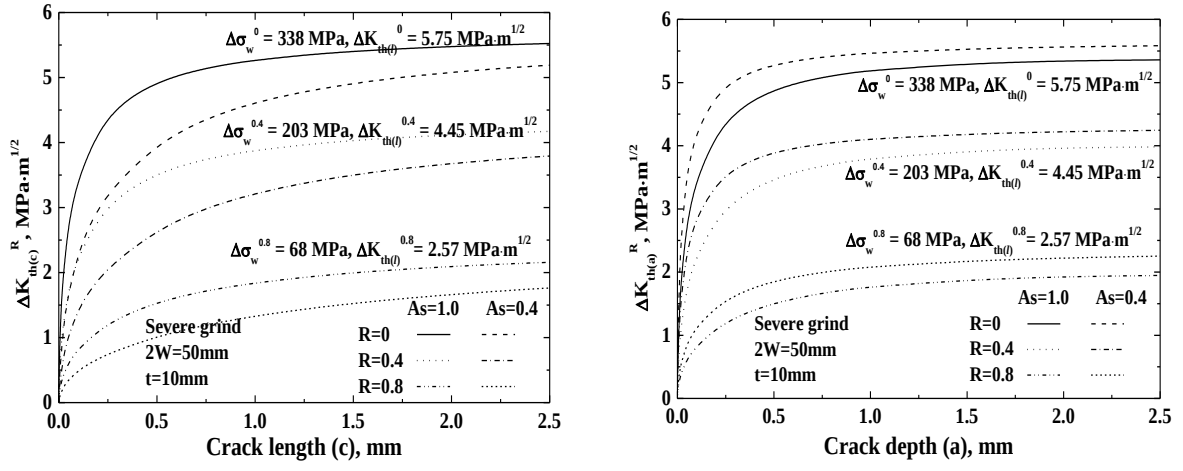

(a) (b)

Fig. 8. Threshold stress intensity factor according crack length (a) and crack depth (b) on severe grind specimen

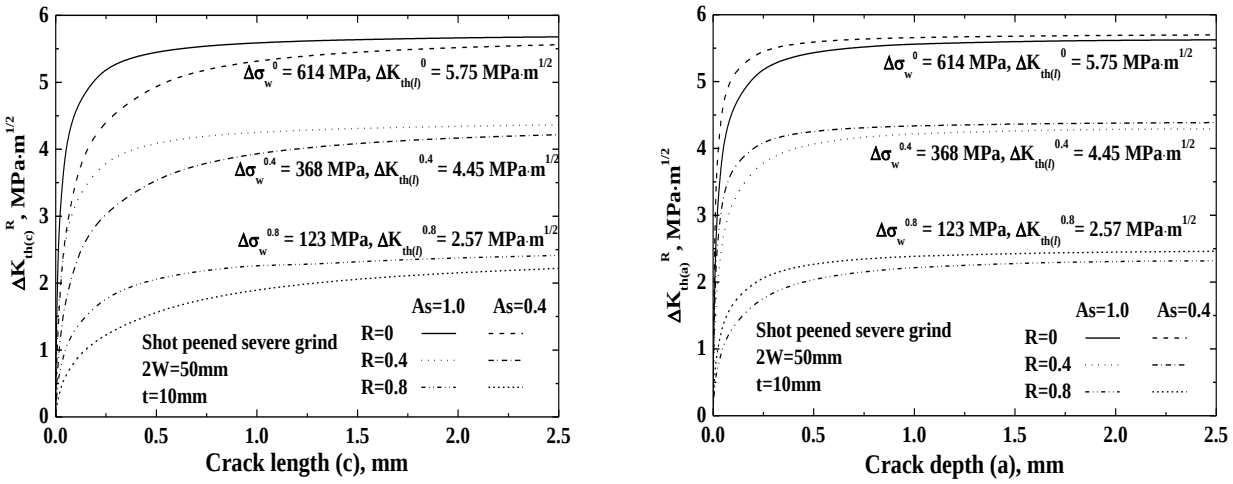

(a) (b)

Fig. 9. Threshold stress intensity factor according crack length (a) and crack depth (b) on shot peened severe grind specimen

5. CONCLUSION

Microdefects inside the materials or in the exterior of a structure develop into cracks over time. Such cracks affect the stability and reliability of the structure, thereby significantly reducing its service life. In this study, the threshold stress intensity factor and the fatigue limit were evaluated according to the stress ratio and the crack aspect ratio, considering the surface cracks generated during the material machining process. The results are as follows.

(1) For the surface cracks of the gentle-grind, severe-grind, and shot-peened severe-grind specimens, the threshold stress intensity factor and the fatigue limit could be evaluated according to the stress ratio and the crack aspect ratio using the equivalent crack length.

(2) As the crack length increased, the fatigue limit decreased, and it decreased more rapidly when the stress ratio (*R*) was lower and the aspect ratio (*As*) was higher. As the crack depth increased, however, the fatigue limit decreased more rapidly when the stress ratio (*R*) was lower and the aspect ratio (*As*) was lower.

(3) As the crack length increased, the threshold stress intensity factor increased, and it increased more rapidly when the stress ratio was lower and the aspect ratio was higher. As the crack depth increased, however, the threshold stress intensity factor increased more rapidly when both the stress ratio and the aspect ratio were lower.

(4) Under the same stress ratio, as the crack length increased, the fatigue limit decreased less rapidly when the aspect ratio was 0.4 than when it was 1.0. As the crack depth increased, however, the fatigue limit decreased more rapidly when the aspect ratio was 0.4 than when it was 1.0. The threshold stress intensity factor, however, increased less rapidly when the aspect ratio was 0.4 than when it was 1.0 as the crack length increased under the same stress ratio. As the crack depth increased, however, the threshold stress intensity factor increased more rapidly when the aspect ratio was 0.4 than when it was 1.0. This is because the crack propagates first in the depth direction rather than in the surface direction when the aspect ratio is high, and it propagates at the same time when it becomes similar to the crack length.

REFERENCES

[1] Frost, N. E., 1957, "Non-propagating cracks in vee-notched specimens subject to fatigue loading", The Aeronautical Quarterly, Vol. 8, Issue 1 , pp. 1−20.

[2] Kitagawa, H. and Takahashi, S., 1976, "Applicability of fracture mechanics to very small cracks or cracks in the early stage. In: Proceedings of the second international conference on mech. Behavior of matls., ASM; pp. 627-631.

[3] El Haddad, M. H., Topper, T. H. and Smith, K. N., 1979, "Prediction of non propagating cracks", Engineering Fracture Mechanics, Vol. 11, Issue 3, pp. 573−584.

[4] Tange, A., Akutu, T. and Takamura, N., 1991, "Relation between shot-peening residual stress distribution and fatigue crack propagation life in spring steel," Transactions of Japan Society of Spring Engineers, Vol. 36, pp. 47−53.

[5] Newman Jr, J. C. and Raju, I. S., 1981, "An empirical stress-intensity factor equation for the surface crack", Engineering Fracture Mechanics, Vol. 15, No. 1-2, pp. 185−192.

[6] Takahashi, K., Hayashi, T., Ando, K. and Takahashi F., 2010, "Evaluation of acceptable defect size by shot peening based on fracture mechanics,"Transactions of Japan Society of Spring Engineers, Vol. 55, pp. 25−30.

[7] Nakagawa, M., Takahashi, K., Osada, T., Okada, H. and Koike, H., 2014, "Improvement in fatigue limit by shot peening for high-strength steel containing crack-like surface defect (Influence of surface crack aspect

ratio),” Transactions of Japan Society of Spring Engineers, Vol. 59, pp. 13−18.

[8] Fueki, R., Abe, H., Takahashi, K., Ando, K., Houjou, K. and Handa, M., 2015 “Harmless by peening for stainless steel containing a crack at the weld toe zone,”High Pressure Institute of Japan, Vol. 53, pp. 30−38.

[9] Yamada, Y., Eto, H., Konya, J. and Takahashi, K., 2018, “Influence of crack-like surface defects on the fatigue limit of nitrocarburized carbon steel,” 2018 International Conference on Material Strength and Applied Mechanics, Vol. 372. pp. 1−6.

doi:10.1088/1757-899X/372/1/012005

[10] Ando, K., Fueki, R., Nam, K. W., Matsui, K. and Takahashi, T., 2019, “A study on the unification of the threshold stress intensity factor for micro crack growth,” Transactions of Japan Society of Spring Engineers, Vol. 64, pp. 39−44.

[11] http://texas-shotpeening.metalimprovement.com/reason_to_shot_peen_metal_fatigue.php

[12] Kobayashi, M., Matsui, T. and Murakami, Y., 1998, “Mechanism of creation of compressive residual stress by shot peening,” International Journal of Fatigue, Vol. 20, pp. 351−357.

[13] Torres, M. A. S. and Voorwald, H. J. C., 2002, “An evaluation of shot peening, residual stress and stress relaxation on the fatigue life of AISI 4340 steel,” International Journal of Fatigue, Vol. 24, pp. 877−886.

[14] Takahashia, K., Osedoa, H., Suzukia, T. and Fukuda, S., 2018, “Fatigue strength improvement of an aluminum alloy with a cracklike surface defect using shot peening and cavitation peening,” Engineering Fracture Mechanics, Vol. 193, pp. 151−161.

[15] Kitsunai, y., 1980, “Effect of microstructure on fatigue crack growth behavior of carbon steels”, The Society of Materials Science of Japan, Vol. 29, pp. 1018−1023.